Electronic Supplementary Information

Facile synthesis of oxygen defective yolk-shell BiO_{2-x} for visible-light-driven photocatalytic inactivation of *Escherichia coli*

Hongli Sun,[a] Ho Yin Yip,[a] Zhifeng Jiang*[ab] Liqun Ye[c], Irene M.C. Lo[d] and Po Keung Wong*[a]

[a]School of Life Science, The Chinese University of Hong Kong, Shatin, New Territories, Hong Kong, China
*E-mail: pkwong@cuhk.edu.hk (PK Wong)

[b]Institute for Energy Research, Jiangsu University, Zhenjiang, Jiangsu, 212013, China
*E-mail: ntjiangzf@sina.com (ZF Jiang)

[c]Engineering Technology Research Center of Henan Province for Solar Catalysis, College of Chemistry and Pharmaceutical Engineering, Nanyang Normal University, Nanyang 473061, China
*E-mail: yeliquny@163.com (LQ Ye)

[d]Department of Civil and Environmental Engineering, Hong Kong University of Science and Technology, Clear Water Bay, Kowloon, Hong Kong SAR, China
*E-mail: cemclo@ust.hk (IMC Lo)

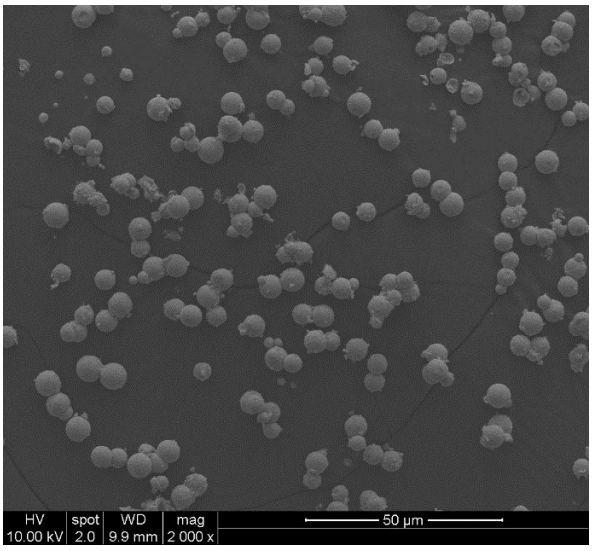

Figure S1. SEM image of yolk-shell BiO_{2-x}.

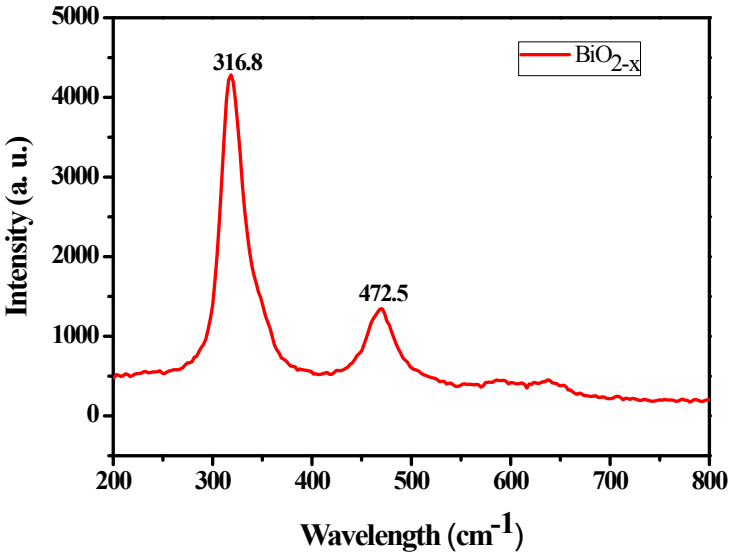

Figure S2. Raman spectra of yolk-shell BiO_{2-x}.

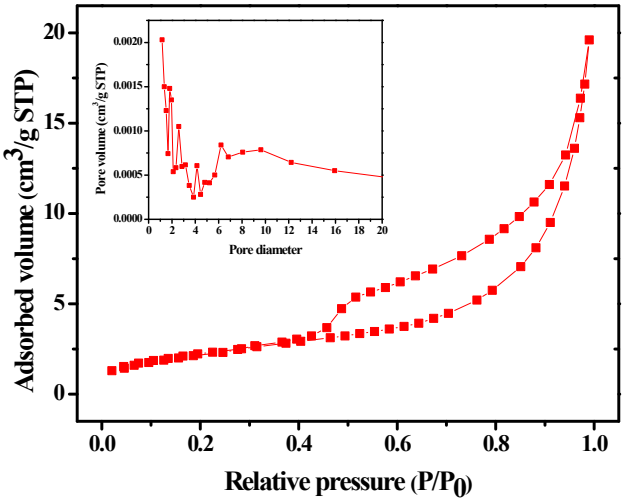

Figure S3. BET pattern of yolk-shell BiO_{2-x}.

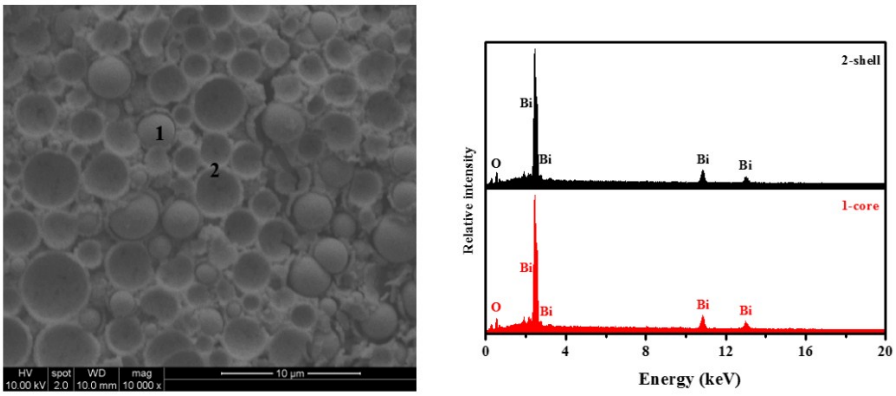

Figure S4. SEM image and corresponding EDX spectra.

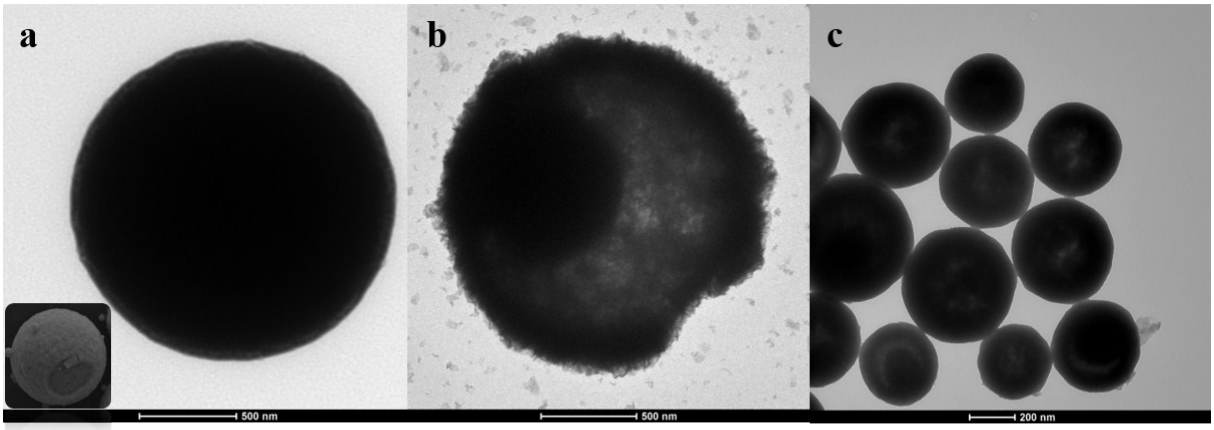

Figure S5. TEM images of BiO_{2-x} with (a) core-shell structure, b) yolk-shell structure, and c) complex hollow structures.

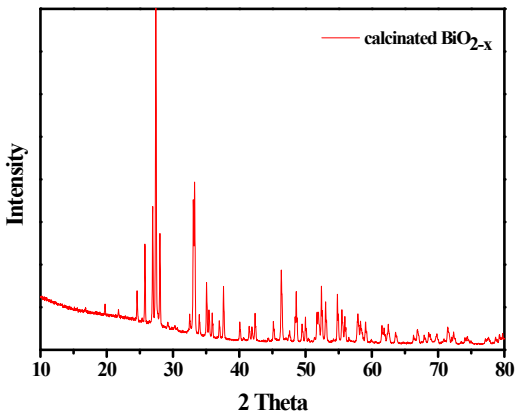

Figure S6. XRD pattern of the calcinated yolk-shell BiO_{2-x} microspheres under 500 °C in air for 4 h.

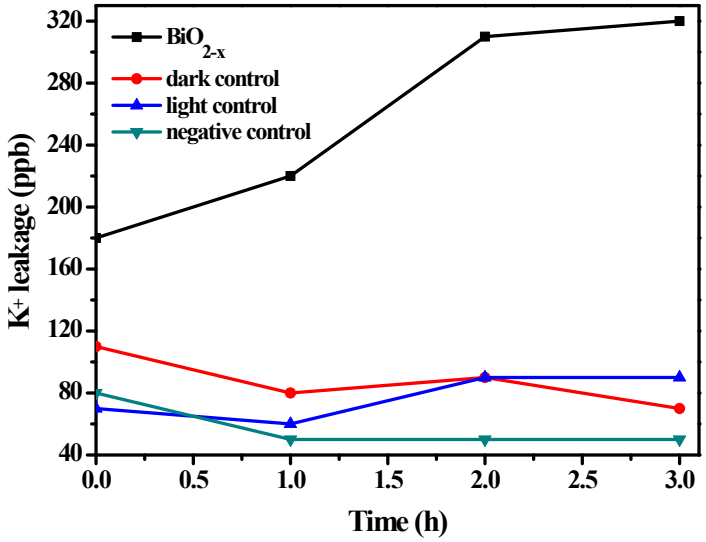

Figure S7. Potassium ion leakage during the photocatalytic inactivation process.

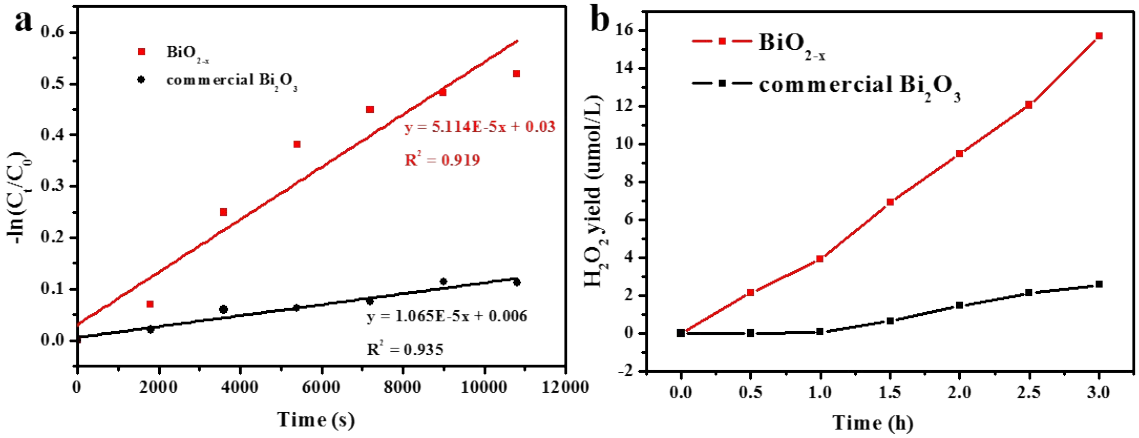

Figure S8. a) Pseudo-first-order reaction fitting curve of NBT concentration, and b) H_2O_2 concentration in the presence of BiO_{2-x} or Bi_2O_3 under visible light irradiation.

Table S1. Element composition of the core and shell of yolk-shell BiO_{2-x} microspheres.

Position	Element	Atom %	Ratio
Core	O	59.43	1.46
	Bi	40.57	
Shell	O	55.36	1.24
	Bi	44.64	

Table S2. Fitted parameters based on Geeraerd proposed model "shoulder + log−linear".

Catalyst	k_{max} (h^{-1})	*S* (h)	*R square*
Yolk-shell BiO_{2-x}	11.16	1.61	0.997
Core-shell BiO_{2-x}	6.85	1.74	0.987
Commercial Bi_2O_3	3.76	0.49	0.994

Table S3. Reaction potentials involved in photocatalytic generation of reactive species.

Eq.	Reactions	Potentials	Reference
2	$O_2 + e_{cb}^- \rightarrow O_2^-$	E = -0.33V	1
3	$O_2^- + H^+ + e_{cb}^- \rightarrow \cdot HO_2$	E = -0.046V	1
4	$\cdot HO_2 + H^+ + e_{cb}^- \rightarrow H_2O_2$	E = 1.44 V	1

Table S4. Surface area, pore volume and pore diameter of the obtained samples.

Catalysts	Surface area (m^2/g)	Pore volume (cm^3/g)	Pore diameter (nm)
commercial Bi_2O_3	0.71	0.002	1.35
core-shell BiO_{2-x}	8.98	0.028	3.83
yolk-shell BiO_{2-x}	15.85	0.033	3.79

References

1. G. H. Moon, W. Kim, A. D. Bokare, N. E. Sung and W. Choi, *Energy Environ. Sci*, 2014, **7**, 4023-4028.